J. Fluid Mech. (1977), *vol.* 81, *part* 3, *pp.* 497–512
Printed in Great Britain

Magnus effect in saltation

By BRUCE R. WHITE AND JAN C. SCHULZ†
Department of Mechanical Engineering, University of California, Davis

(Received 18 August 1976)

High-speed motion pictures (2000 frames/s) of saltating spherical glass microbeads (of diameter 350–710 μm and density 2·5 g/cm^3) were taken in an environmental wind tunnel to simulate the planetary boundary layer. Analysis of the experimental particle trajectories show the presence of a substantial lifting force in the intermediate stages of the trajectories. Numerical integration of the equations of motion including a Magnus lifting force produced good agreement with experiment. Typical spin rates were of the order of several hundred revolutions per second and some limited experimental proof of this is presented. Average values and frequency distributions for lift-off and impact angles are also presented. The average lift-off and impact angles for the experiments were 50° and 14° respectively. A semi-empirical procedure for determining the average trajectory associated with given conditions is developed.

1. Introduction

A sufficiently strong wind blowing over a sandy surface will pick up sand grains and cause them to skip along the surface in a series of short flat trajectories. At each impact these bounding grains may eject other grains, which in turn will begin to hop across the surface. The net result will be flow of sand in the direction of the wind. This phenomenon is known as saltation. The term was first applied to the movement of sand under water in a paper by Gilbert (1914) and comes from the Latin verb *saltare*, which means 'to leap or dance'.

Saltation is of interest from a geological point of view because it is the mechanism primarily responsible for the unique topography of sandy desert regions. Dunes, ridges, ripples and similar features all owe their existence and continual movement to the action of the wind. Recently interest in saltation has increased because of evidence in the form of pictures sent back by the *Mariner* and *Viking* spacecraft that it is perhaps an even more important geological force on the surface of Mars.

The classic work on the subject of saltation is the remarkable book by Bagnold (1941). Drawing on his years of study of saltation occurring in the Sahara and other desert regions as well as on the results of wind-tunnel tests, Bagnold describes in both quantitative and qualitative terms the phenomenon of saltation as it was then understood. His book has had a profound influence on subsequent research in this area.

The purpose of the present investigation was to learn more about the trajectories of saltating grains through the study and evaluation of high-speed motion-picture films taken in an atmospheric wind tunnel. The saltating material was glass spheres with a density of 2·5 g/cm^3. Four types of sphere, each with a different diameter range, were photographed at several flow velocities. The films were taken at a nominal frame

† Present address: Detonation Physics Department, Naval Weapons Laboratory, China Lake, California 93555.

speed of 1000 or 2000 frames/s, the higher speed being used for the higher flow velocities. Trajectory data were gathered from the films with the help of a Vanguard Motion Analyzer.

2. Saltation theory

Threshold friction velocity

It is a matter of experience that a gentle wind blowing over a sandy surface will not cause movement of the sand grains. The minimum friction velocity at which the flow has sufficient energy to lift grains off the surface and thereby initiate saltation is known as the threshold friction velocity. Based on an evaluation of the relevant parameters, Bagnold derived an expression for the threshold friction velocity u_{*t} of the form

$$u_{*t} = A(\rho_p g D_p/\rho)^{\frac{1}{2}}, \tag{1}$$

where ρ is the fluid density, ρ_p the particle density, D_p the particle diameter and g the acceleration due to gravity. The dimensionless quantity A was assumed by Bagnold to be a function of only the friction Reynolds number $R_f = u_* D_p/\nu$, where ν is the kinematic viscosity.

For values of R_f greater than about 5, A in air is nearly constant with a value of 0·118 (Iversen *et al.* 1976). For values of R_f less than 5, A increases rapidly with decreasing R_f. This behaviour is probably due to the presence at low friction Reynolds numbers of a viscous sublayer which, in effect, shields the surface from turbulent fluctuations present in the flow. For particles of small diameter it is likely that cohesive forces, possibly due to adsorbed water films, also contribute to the higher A values. A more complete discussion of the threshold determination as well as empirical equations and graphs for obtaining A can be found in Iversen *et al.* (1976).

Velocity profiles

A one-dimensional flow situation is assumed in which the velocity in the vertical (y) direction is zero and the velocity u in the flow (x) direction is a function of height above the surface only. The flow geometry and a typical velocity profile are shown on figure 1.

In the absence of saltation (i.e. for friction velocities below the threshold friction velocity or at higher friction velocities for non-erodible surfaces), if the flow is fully turbulent the boundary layer will have a logarithmic velocity profile given by

$$\frac{u}{u_*} = \frac{1}{k}\ln\left(\frac{y}{y_0}\right), \tag{2}$$

where u_* is the friction velocity, y_0 the roughness height and k von Kármán's constant. For a surface of like particles the roughness height may be taken equal to $\frac{1}{30}D_p$ (Monin & Yaglom 1965) and von Kármán's constant as 0·4, so that this equation becomes

$$\frac{u}{u_*} = 2{\cdot}5\ln\left(\frac{y}{D_p}\right) + 8{\cdot}5. \tag{3}$$

The presence of saltation significantly alters the nature of the velocity profiles as illustrated on figure 2, which is a plot of the logarithm of the height *vs.* velocity with

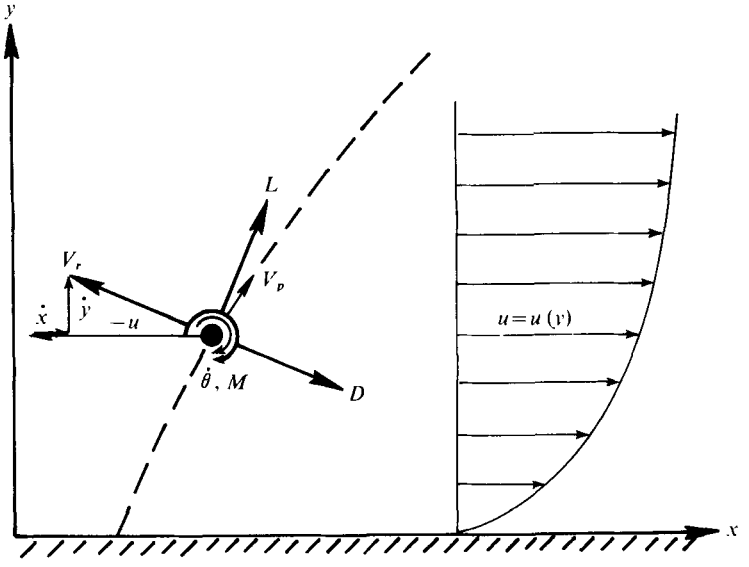

FIGURE 1. Forces and velocities associated with a saltating particle.

friction velocity as a parameter for both saltating and non-saltating flows over the same surface. For the non-saltating flow the height–velocity lines (obtained from (3) and shown solid on the figure) are straight and converge to a focus at the roughness height y_0, where the velocity is zero. For the saltating flows, as has been demonstrated experimentally by Bagnold and others, the height–velocity lines (dashed on the figure) are also straight, but converge to a different focus at some greater height y_0' and non-zero velocity u_0'. The lines corresponding to the same u_* for saltating and non-saltating flows respectively have the same slope. Therefore the velocity-profile equation for saltating flows can be written from the figure as

$$\frac{u}{u_*} = 2{\cdot}5 \ln\left(\frac{y}{y_0'}\right) + \frac{u_0'}{u_*}. \tag{4}$$

According to Bagnold the focus for saltating flows lies on the height–velocity line corresponding to the threshold friction velocity u_{*t}. Moreover, this particular line is the same whether saltation is occurring or not (i.e. the solid and dashed lines for $u_* = u_{*t} = 38$ cm/s coincide on the figure). Hence from (3)

$$\frac{u_0'}{u_{*t}} = 2.5 \ln\left(\frac{y_0'}{D_p}\right) + 8{\cdot}5. \tag{5}$$

The height y_0' of the saltating focus is a function primarily of the diameter of the saltating particles. On the basis of an examination of pertinent experimental data, Andres (1970) concluded that this size dependence can be adequately modelled by taking y_0' equal to $2{\cdot}5D_p$. Substitution of this relationship and (5) into (4) yields the final form of the velocity-profile equation for saltating flows:

$$\frac{u}{u_*} = 2{\cdot}5 \ln\left(\frac{y}{D_p}\right) - 2{\cdot}29 + 10{\cdot}79 \frac{u_{*t}}{u_*}. \tag{6}$$

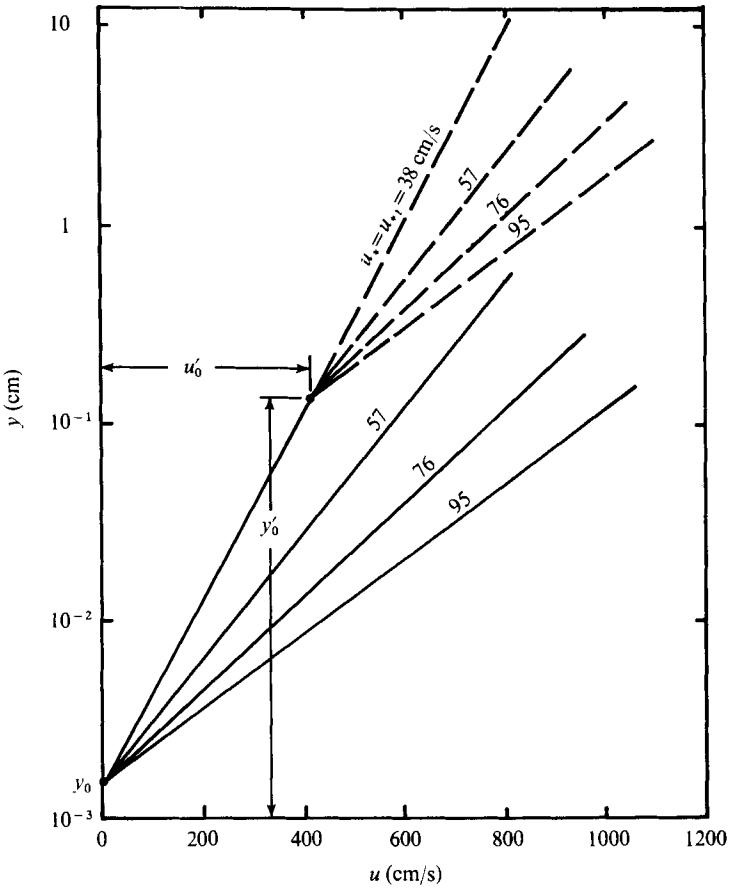

FIGURE 2. Theoretical height as a function of velocity for saltating flows (dashed lines) and for non-saltating flows (solid lines) for friction speeds of 38, 57, 76 and 95 cm/s. D_p = 0·05 cm, u_{*t} = 38 cm/s.

As u_* approaches u_{*t} this equation approaches the equation (3) for a fully developed, non-saltating turbulent boundary layer. It seems unlikely that a viscous sublayer could exist in a saltating flow because the particles continually leaving and returning to the surface would break up any such layer that tried to form. Consequently, (6) should be valid for all friction Reynolds numbers, even those extending into the transition and viscous-sublayer ranges.

Equations of Motion

The forces acting on a saltating particle tending to change its state of motion are a downward force due to its weight and aerodynamic forces produced by the fluid flowing past it. The latter can be resolved into an equivalent lift force L, drag force D and moment M, as shown in figure 1. The direction of the drag force is opposite to the direction of V_r, the velocity of the particle relative to the flow.

The equations for the translational and rotational motion of a particle can be written as

$$m_p \ddot{x} = L\frac{\dot{y}}{V_r} - D\frac{\dot{x}-u}{V_r}, \tag{7}$$

$$m_p \ddot{y} = -L\frac{\dot{x}-u}{V_r} - D\frac{\dot{y}}{V_r} - m_p g, \tag{8}$$

$$I_p \ddot{\theta} = M, \tag{9}$$

where m_p is the particle's mass, I_p the particle's moment of inertia, $\ddot{\theta}$ the particle's angular acceleration and $(\dot{x}, \dot{y})$ and $(\ddot{x}, \ddot{y})$ are the particle's velocity and acceleration components, respectively.

The magnitude of the relative velocity can be expressed in terms of the particle and flow velocities as

$$V_r = [(\dot{x}-u)^2 + \dot{y}^2]^{\frac{1}{2}}. \tag{10}$$

It has generally been assumed by previous researchers that the drag force is the primary fluid force acting on a saltating particle and that the lift force and moment can be neglected except at very small heights where the influence of the surface becomes important (White 1975). The effect of drag is customarily expressed in terms of the drag coefficient C_D, defined by

$$D = \tfrac{1}{2} C_D A_p \rho V_r^2, \tag{11}$$

where A_p is the particle's cross-sectional area.

If the particles are assumed spherical and of uniform density, then the equations of motion including only the drag force simplify to (White *et al.* 1976)

$$\ddot{x} = -\frac{3}{4}\frac{\rho}{\rho_p}\frac{V_r}{D_p} C_D(\dot{x}-u), \tag{12}$$

$$\ddot{y} = -\frac{3}{4}\frac{\rho}{\rho_p}\frac{V_r}{D_p} C_D \dot{y} - g. \tag{13}$$

Drag coefficient

The drag coefficient of a sphere is strongly dependent on the Reynolds number. A number of empirical representations for this dependence have been developed. Perhaps the best of these is given in the paper by Morsi & Alexander (1972), who derived a set of equations expressing the relationships between the drag coefficient and Reynolds number over the entire Reynolds number range. Their equations were used to calculate the drag coefficients needed in the numerical integrations performed in the present research.

3. Comparison of filmed and theoretical trajectories

The high-speed motion-picture films of saltating flows evaluated in this study were taken with a HiCam camera in an environmental wind tunnel with a test section 1·1 m^2 by 7 m and a speed capability of 40 m/s. The camera was pointed horizontally and perpendicular to the direction of the flow such that the flow and the saltating particles travelled from left to right across successive frames. The flow was lit from above by a thin strip of high intensity light so that only relatively few particles in the direction transverse to the flow direction were illuminated and hence visible on the film. A centimetre grid placed on the far side of the flow provided a spatial reference frame which permitted subsequent determination of the position of individual particles.

The saltating material was glass spheres (silicon-coated microbeads) with a density of 2·5 g/cm^3. Four different types of spheres, each with a different diameter range, were used and each of these types was photographed at several different flow velocities. The films were taken at a nominal frame speed of 1000 or 2000 frames/s, the higher frame speed being used to photograph the higher velocity flows. A strobe light device left a light flash on the margin of the film which permitted a more precise determination of the film speed to be made later.

Before each filmed run, a layer of glass spheres was spread on the wind-tunnel floor, carefully smoothed out and levelled to a height of about 1 cm. The patch covered was approximately 10 cm by 200 cm, the longer dimension being in the direction of the flow. The flow friction velocity and free-stream velocity during the runs were determined by measuring the pressure differential between the inside and outside of the tunnel, the relationship between these velocities and the pressure differential having been established previously from velocity traverses made with no 'sand' in the tunnel. The air density based on atmospheric conditions at the time of the runs was 0·00124 g/cm^3.

A preliminary viewing of the film on a standard 16 mm projector revealed many of the qualitative characteristics of the saltation process. The particles could be seen leaving the surface at relatively high angles, being turned and accelerated horizontally by the flow, and then impacting with the surface again at relatively shallow angles. (Actually, there was considerable variation in the lift-off and impact angles and velocities and in the trajectory heights and lengths for individual particles.) For a given type of material the height of the saltation layer and the amount of material being moved were observed to increase with increasing flow friction velocity. In fact, the intensity of the saltation increased so much that it became virtually impossible in the higher velocity runs to observe individual particles. This was especially true near the surface, where the mass flux of saltating material was greatest.

An interesting phenomenon was observed for the spheres of smallest diameter (5–53 μm) at high flow friction velocities. More dense and less dense clouds of saltating particles could alternately be seen sweeping horizontally across the frames, so that the intensity of the saltation appeared to vary with time in an approximately periodic manner. The fluctuations in intensity occurred so rapidly that they were made visible only through the use of high-speed photography. Apparently, this phenomenon has not been reported previously in the literature, and no explanation for it is known.

In order to obtain trajectories of individual saltating particles, the film was analysed using a Vanguard Motion Analyzer. The film could be run through this instrument forwards or backwards either at a continuously variable speed or frame by frame. A frame counter made it possible to keep track of position within the section of film being viewed. The film was projected onto a flat frosted-glass surface, the size of the projected image on this surface being about 5 cm by 9 cm. Crank-operated horizontal and vertical cross-hairs could be centred on any point on the screen, and its position read from dials to within one-thousandth of an inch (25·4 μm).

A number of trajectories were collected from the film. These were compared with theoretical trajectories obtained by numerical integration of the equations of motion including only the drag force [(12) and (13)] with starting values for the integration chosen as the initial position and velocity of the particles on the filmed trajectories. The outcome in a typical case is shown in figure 3.

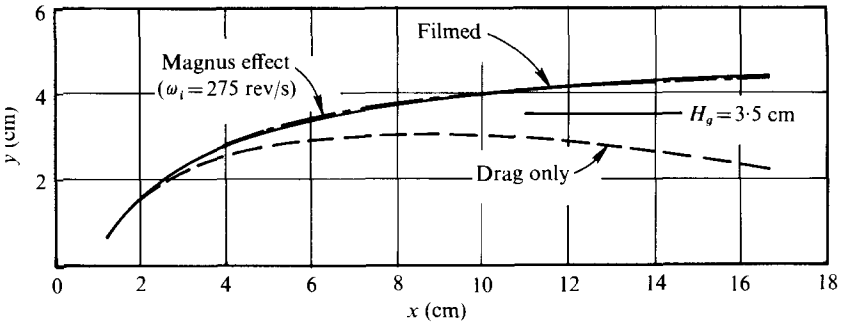

FIGURE 3. A comparison of a filmed (solid line) path traced out by a particle with theoretical calculations (dashed lines) from the equations of motion with and without a particle spin rate of 275 rev/s. Also shown is the maximum height H_g possible in the absence of all forces except gravity. D_p = 350–710 μm, $u_* = 39.6$ cm/s.

It can be seen that the agreement between theory and experiment is poor. The filmed particle reached a much greater height (over 50 % greater before it had quite reached the top of its trajectory) than the theoretical one. If the drag force were zero and the particle acted on only by gravity, the maximum height it could attain is given by

$$H_g = y_i + V_{yi}^2/2g, \tag{14}$$

where y_i and V_{yi} are the height and vertical component of velocity of the particle at the initial point on the trajectory.

The filmed particle, however, rose considerably above even this no-drag height, which is indicated on the figure. If anomalies in the experimental data (which seem unlikely) are absent, it would appear that, in addition to the drag force, there must also be a substantial lift force acting on the particle to account for its observed behaviour.

The most plausible source of this additional lift is the Magnus effect associated with rotation of the particle. Rubinow & Keller (1961) have derived the following expressions for the Magnus lift force and moment acting on a rotating sphere:

$$L = \tfrac{1}{8}\pi D_p^3 \rho V_r(\dot{\theta} - \tfrac{1}{2}\partial u/\partial y), \tag{15}$$

$$M = \pi\mu D_p^3(\dot{\theta} - \tfrac{1}{2}\partial u/\partial y), \tag{16}$$

where $\dot{\theta}$ is the particle's angular velocity and μ the fluid viscosity.

These equations are valid only for the case of vanishingly small Reynolds number. Their use in the present case is justified by the fact that it is desired primarily to find out whether the addition of terms accounting for the Magnus effect will significantly improve the agreement between theory and experiment. The exact value of the terms is not critical so long as they are of the right order of magnitude.

With the inclusion of these lift and moment terms, the general equations of motion (7)–(9) can be integrated to yield new theoretical trajectories accounting for the Magnus effect. Different initial values for the spinning rate were tried until good agreement with the filmed trajectories was obtained. These spinning rates ranged from about 100 to 300 rev/s for the particles considered.

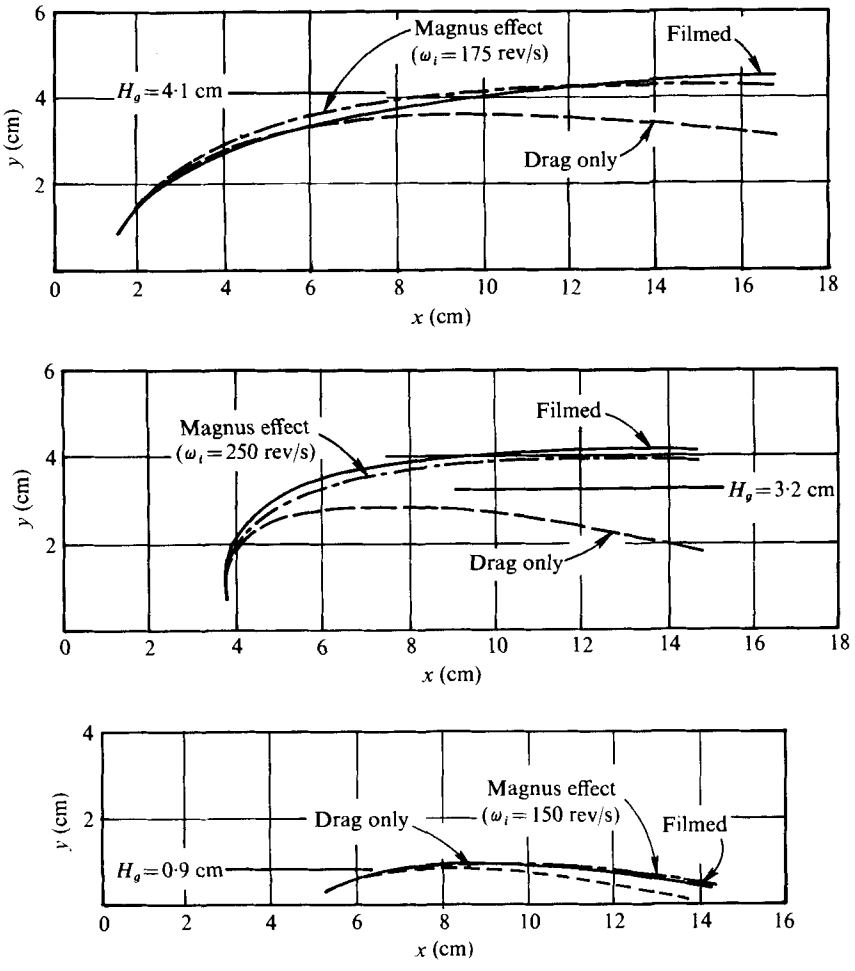

FIGURE 4. A comparison of a filmed (solid line) path traced out by a particle with theoretical calculations (dashed lines) from the equations of motion with and without a particle spin rate of (*a*) 175 rev/s, (*b*) 150 rev/s and (*c*) 250 rev/s. Also shown is the maximum height H_g, possible in the absence of all forces except gravity. D_p = 350–710 μm, $u_* = 39{\cdot}6$ cm/s.

For the particle of figure 3, the theoretical trajectory corresponding to an initial spinning rate of 275 rev/s produced good agreement between theory and experiment. This trajectory is also shown on the figure. (It lies so close to the filmed trajectory that the two form almost a single line.) Similar sets of trajectories for three other particles are shown on figures 4 (*a*)–(*c*). The improvement in agreement between theory and experiment is not always as pronounced as in figure 3. Nevertheless, it is apparent that inclusion of the Magnus effect in the equations of motion resulted in trajectories that are in substantially better agreement with the filmed trajectories for all these particles.

The particle spinning rates of 100–300 rev/s required to produce this better agreement seem rather high. Because these rates could not be uniformly observed on the film, there are no corresponding experimental measurements of the spin rates for the trajectories presented. There is, however, at least partial confirmation of them.

As reported in Torobin & Gauvin (1959, 1960), observations of freely moving spheres suggest that the ratio of peripheral velocity to the mean velocity relative to the flow should be of the order of 5 %. For the filmed flow from which the previous particle trajectories were obtained, the free-stream velocity was about 1030 cm/s. If the mean velocity is taken as half this value and the average particle diameter as 530 μm, the spinning rate comes out to be 155 rev/s.

It was noticed in the present study that some of the particles appeared to undergo a periodic change in brightness as they travelled across the film frames. This blinking behaviour may be due to the fact that the particles are spinning in such a way that flat spots on their surfaces are reflecting light back towards the camera more strongly once each revolution. By observing a number of these blinking particles and counting the number of flashes during the period of observation, it was possible to estimate the spinning rates for these particles. These ranged from 115 to 500 rev/s, the average being 320.

It does not appear to be unusual for a seemingly high spin ratio to occur for saltating particles. Chepil (1945) was one of the first investigators to find particle spinning rates. Photographs were taken of soil moving in saltation. Chepil reports that these photographs 'indicate that grains carried in saltation rotate at a speed of 200 to 1000 revolutions per second'. Chepil further explains that the photographs clearly show that 50 % or more of the grains spin and another 25 % or so have relatively indistinct rotation. He also states that these percentages may be low owing to the type of illumination that was used. From his observations of the nearly vertical rise of grains leaving the surface Chepil concludes that the only logical explanation of this occurrence is the presence of substantial lifting forces. These forces are caused by the Magnus effect as well as the steep velocity gradient.

Francis (1973) realized the importance of the spinning of particles to saltation. He states that its effect is to enhance lifting forces in the initial stages of the particle trajectory and to curtail motion in the final phase. Also mentioned is the lack of experiments performed to determine the magnitude of these forces on naturally rough grains in shear flows. Francis states that 'studies on this point might prove valuable to explain the beginning and ending of the trajectories'. The authors feel that the entire particle trajectory is altered with significantly high spin rates. Francis does account for spin in his analysis of particle motion along the bed of a water stream.

Many investigators have shown the importance of lifting forces in saltation. Einstein & El-Samni (1949), Chepil (1958), Bagnold (1973), Francis (1973) and Tsuchiya (1970) have all shown that the presence of a lifting force is necessary to initiate motion of grains as well as to maintain their motion in a saltating process. Although no qualitative division was performed on the relationship of Magnus to pressure lift forces during the saltation process, it appears that the Magnus force is substantial when a particle collides with the surface and is ejected from it. Here the spinning rates of the particles appear to be highest. As the particle progresses along its trajectory the spinning rate appears to decrease and be smaller when the particle collides with the surface. The spinning rate is generally increased by a collision with the surface.

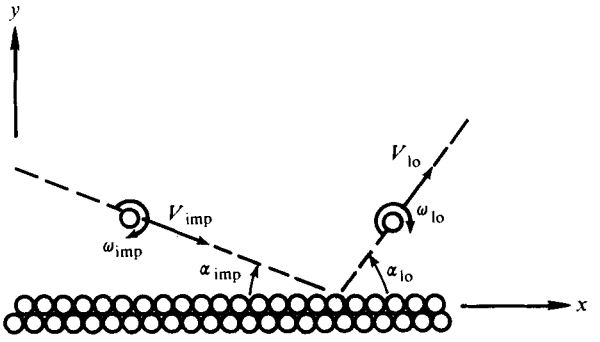

FIGURE 5. Geometry of lift-off angle α_{lo}, impact angle α_{lmp} and impact velocities for a particle colliding with a surface consisting of like particles.

4. Average lift-off and impact angles and velocities

An approximate technique was used to obtain average lift-off angles α_{lo}, and impact angles α_{lmp}, and the corresponding velocities and frequency distributions from the films. The geometry of the angles is presented in figure 5. Basically, this technique involved the random selection of a large number of particles lying between about half and three-quarters of a centimetre above the surface. (The paths of particles closer to the surface could not be followed consistently because of visual interference from clouds of other particles.) Three points along the paths of each of these particles were obtained so that their trajectories could be extrapolated parabolically back to the surface to determine their lift-off or impact angles and velocities.

Since this technique in effect ignores particles with trajectory heights less than half to three-quarters of a centimetre, it cannot give true averages and distributions for all particles leaving or returning to the surface. Nevertheless, it is felt that the averages and distributions obtained do not differ greatly from the true ones.

The results obtained by applying this technique to one of the filmed flows are summarized in figures 6 (*a*) and (*b*), which give averages and frequency plots for the lift-off and impact angles and velocities respectively. The following comments can be made concerning these plots.

(i) The distributions of impact angles and velocities appear to be approximately normal (bell shaped). The lift-off distributions, on the other hand, are considerably skewed.

(ii) Of the hundred particles looked at, considerably more were lifting off than impacting (57 *vs.* 43), indicating that the selection of particles was not completely random, since in that case there would have been an equal (or more nearly equal) number of ascending and descending particles. It is possible that more lifting-off particles were selected because they were moving more slowly and tended to make sharper, more distinct images on the film. The faster-moving impacting particles, on the other hand, may have appeared slightly blurred and been less noticeable.

(iii) There is little data available with which to compare these results. The average impact angle (13·9°) is within the range of 10–16° suggested by Bagnold. On the other hand, the wide range of lift-off angles and the relatively low average value (49·9°) are at variance with a statement of Allen (1970, p. 98) that 'The initial rise of a saltating grain is directed almost vertically up from the bed'.

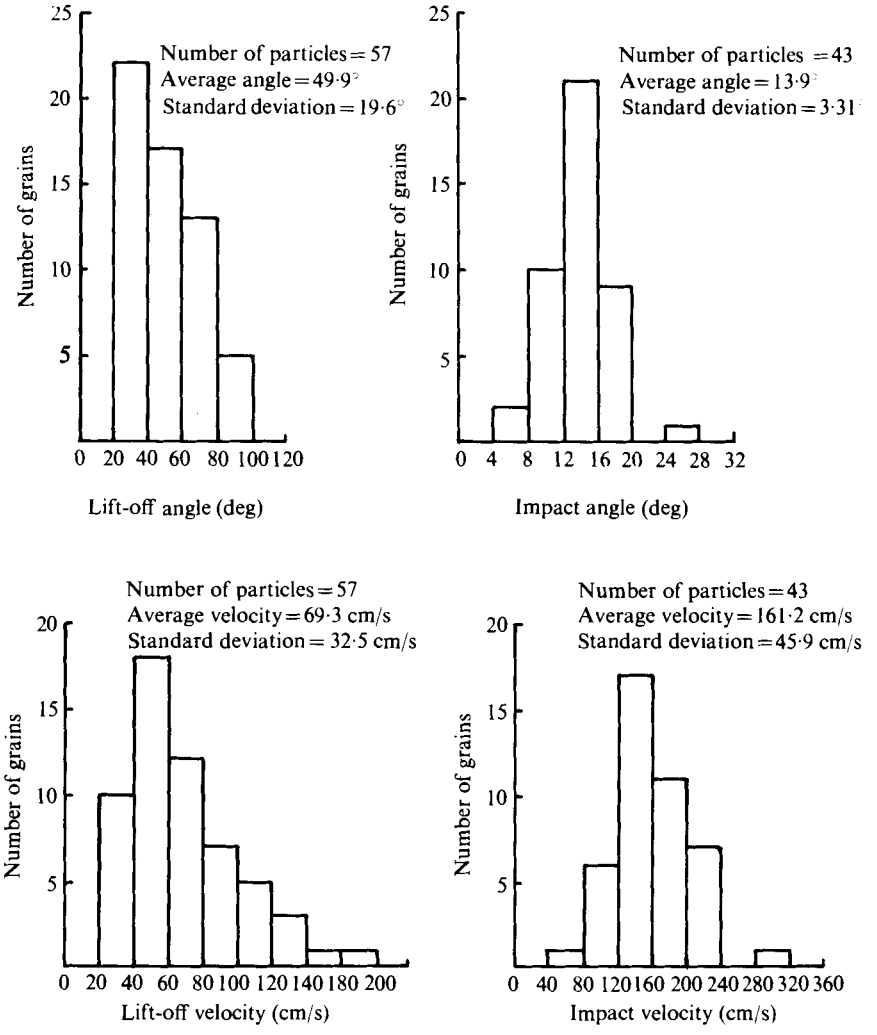

FIGURE 6. Distributions and average values of (*a*) lift-off and impact angles and (*b*) lift-off and impact velocities from filmed saltating trajectories for flow with a constant friction speed of 39·6 cm/s. Total number of particles = 100.

5. Analytical determination of average trajectories

It has been assumed by various researchers starting with Bagnold that associated with every saltating flow there is an average or typical trajectory which represents the path most nearly followed by the majority of particles. In this section the development of an analytical procedure for determining this average trajectory will be described. Because our theoretical understanding of the saltation process is at present incomplete this procedure will also be incomplete and its limitations will be pointed out.

In order to determine average trajectories analytically it is necessary to be able to solve two problems: *the trajectory problem*, that is, given the lift-off state of a particle (i.e. its lift-off angle, velocity and rotational speed) calculate its trajectory through the flow; *the impact problem*; that is, given a particle approaching the surface with a certain

impact angle, velocity and rotational speed, calculate the average lift-off angle, velocity and rotational speed with which it will leave the surface after impact. (Instead of rebounding from the surface itself, the impacting particle may cause another particle or particles to be ejected; or the impacting particle may simply bury itself in the surface with no particle being ejected. On the average, however, something must rebound from the surface at some average angle, velocity and rotational speed, otherwise the saltation could not continue.)

The first of these problems (the trajectory problem) can be handled easily by numerical integration of the equations of motion for a particle as has previously been described. The solution to the second problem (the impact problem) is not so straightforward and will be discussed in some detail. During impact a particle collides with the similar particles making up the surface. In the process it transfers a portion of its kinetic energy to these other particles. It (or possibly some other particle or particles) then rebounds from the surface with a lift-off velocity that is much lower than the velocity just prior to impact.

Impact with the surface occurs during a very short time interval and is accompanied by extremely high impulsive forces. These will be much larger than forces due to gravity or the fluid. Consequently, it can be assumed that the latter will have little influence on the impact momentum transfer and can be neglected. If, in addition, it is assumed that the saltating particles are sand or other material with about the same density and elastic properties as sand, that they are spherical and smooth, that the packing geometry is similar in all flow situations, that there are no cohesive forces between particles, and that the initial collisions between particles are essentially elastic, then the relationships between the impact and lift-off states can be expressed as

$$V_{1o} = V_{1o}(V_{1mp}, \alpha_{1mp}, \omega_{1mp}), \tag{17}$$

$$\alpha_{1o} = \alpha_{1o}(V_{1mp}, \alpha_{1mp}, \omega_{1mp}), \tag{18}$$

$$\omega_{1o} = \omega_{1o}(V_{1mp}, \alpha_{1mp}, \omega_{1mp}), \tag{19}$$

where V_{1o} is the lift-off velocity, V_{1mp} is the impact velocity, α_{1mp} is the impact angle, ω_{1mp} is the impact rotational speed (in rev/s), α_{1o} is the lift-off angle and ω_{1o} is the lift-off rotational speed. The geometry of the impact situation defining these quantities is shown on figure 5.

Unfortunately, there appears to be little information available in the literature which can be used to determine the explicit form of the functional relationships indicated above. However, in order to illustrate the analytical procedure for determining average trajectories, simple expressions for these relationships will be assumed which are based in part on the data on the average lift-off and impact angle and velocity given in § 4. These relationships are

$$V_{1o} = 80[1 - \exp(-\tfrac{1}{80}V_{1mp})], \tag{20}$$

$$\alpha_{1o} = 21{\cdot}8\,\alpha_{1mp}^{0.316}, \tag{21}$$

$$\omega_{1o} = \frac{V_{1o}}{2\pi D_p}\cos\left(\frac{\alpha_{1o} + \alpha_{1mp}}{2}\right). \tag{22}$$

In deriving these relationships the lift-off velocity was assumed to be a function of the impact velocity only. It was further assumed that the ratio of lift-off to impact

velocity should approach unity as the impact velocity approaches zero and that the lift-off velocity should not increase unboundedly with increasing impact velocity but should approach some limiting maximum value. The decaying exponential relationship given satisfies these assumptions and also agrees with the film data. The lift-off angle was assumed to be a function of the impact angle only. Moreover, it was assumed that a particle impacting vertically would on the average rebound vertically, while a particle impacting horizontally would rebound horizontally. The power-law expression given meets these requirements and also agrees with the film data. The lift-off rotational speed was determined by formulating an expression for the maximum possible rotational speed of a particle leaving the surface while maintaining frictional contact (no slip) with the particles touching it. This expression was then divided by a factor of two to account empirically for the fact that there may actually be some slip.

The existence of an average trajectory implies that the particles will tend to favour this particular trajectory over all others. That is, a particle executing a trajectory larger (or smaller) than average will on the average lose a larger (or smaller) part of its energy on impact, so that its next trajectory will be closer to average. This suggests that average trajectories can be determined by an iterative procedure which involves following a typical particle through a series of trajectories as it approaches the average one.

In this procedure initial lift-off conditions are assumed for the particle at the start of the first trajectory. This first trajectory is then calculated by solving the trajectory problem. Using the impact velocity, angle and rotational speed for this trajectory, lift-off values for these quantities at the start of the next trajectory can be calculated from (20), (21) and (22), the solution to the impact problem. A new trajectory can be calculated using the new lift-off values. These steps can be repeated until the procedure converges to the average trajectory.

This iterative procedure was carried out with the help of the computer and average trajectories were obtained for a number of saltation situations. The results are shown on figures 7, 8 and 9, which are plots respectively of the lift-off and impact angle, the vertical component of the lift-off and impact velocity, and the trajectory height and length *vs.* particle diameter at constant friction velocity ($u_* = 38$ cm/s). The following comments can be made about these plots.

(i) The constant friction velocity of 38 cm/s for which the plots were prepared corresponds to the threshold friction velocity for 500 μm particles. This means that particles larger than 500 μm cannot saltate at this friction velocity. In other words, the velocities and trajectory heights and lengths for particles larger than 500 μm would all be zero if drawn on the figures. It can be seen from the figures that the magnitude of the saltation does not die away gradually towards zero as the cut-off point is approached and then suddenly drop to zero. It is not clear what kind of behaviour occurs in actual saltation situations.

(ii) Equation (20), which gives the lift-off velocity in terms of the impact state, was obtained by fitting a decaying exponential curve to a single film data point. Thus this curve is not really pinned down for larger velocities and may result in substantial error when extrapolated to the extremely high velocities. A sensitivity analysis indicates that the results obtained are strongly dependent on the value of the numerical constant (80) used in this expression.

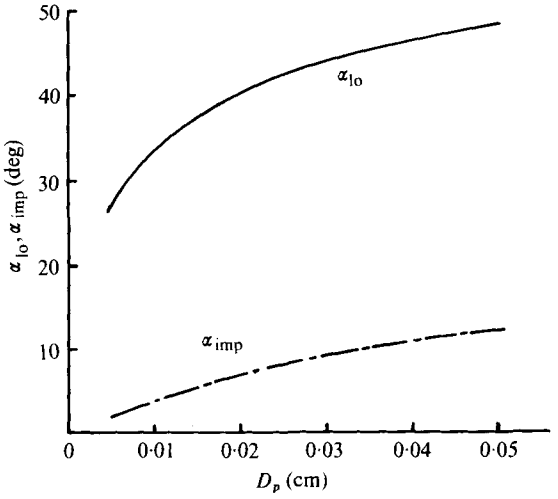

FIGURE 7. Lift-off and impact angles for average particle trajectories as a function of the particle diameter D_p for a constant friction speed of 38 cm/s. These are final average values predicted from an iterative numerical solution of the equations of motion.

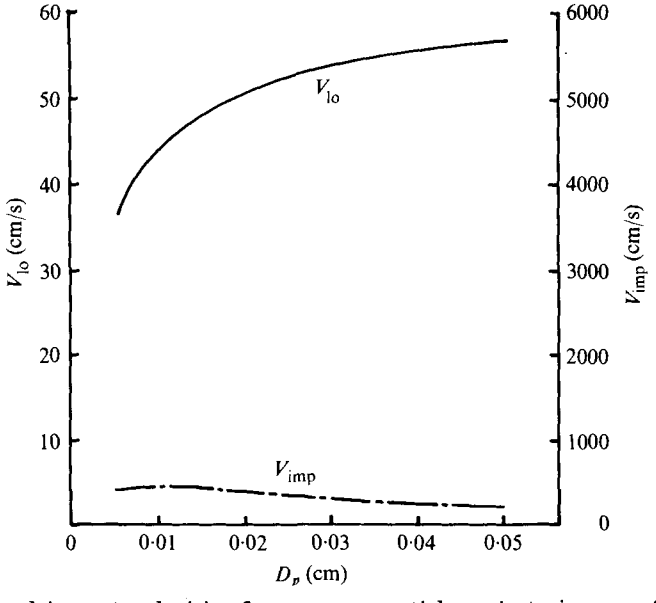

FIGURE 8. Lift-off and impact velocities for average particle trajectories as a function of the particle diameter D_p for a constant friction speed of 38 cm/s. These are final average values predicted from an iterative numerical solution of the equations of motion.

An interesting paper by Ellwood, Evans & Wilson (1975) calculates the mean grain jump length and a corresponding terminal velocity in estimates of sand ripple wavelengths. Ellwood *et al.* performed rebound experiments on granular sand and determined empirical curve fits to the impact and rebound velocities. Although it is difficult to make a direct comparison with their data, the form of the equation relating these velocities appears to be the same, however the constants do vary. The results displayed in figure 9 for the lengths of grain paths do tend to agree with those

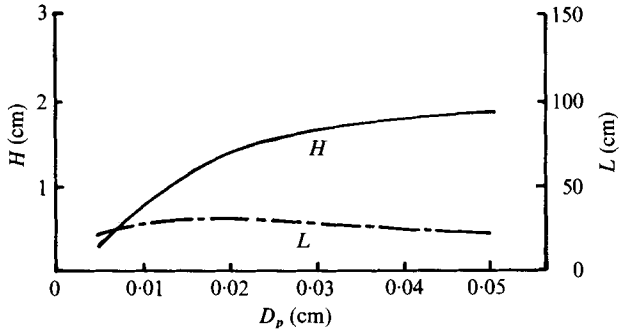

FIGURE 9. Height H and length L of average particle trajectories as a function of the particle diameter D_p for a constant friction speed of 38 cm/s. These are final average values predicted from an iterative numerical solution of the equations of motion.

calculated by Ellwood *et al.* Another saltation grain-trajectory analysis was performed by Zingg (1953).

All of the above analyses and predictions of this paper were for the case of a constant friction speed. If the friction speed (surface shear) were increased the spinning rates of the particles would certainly increase but it would be difficult to estimate the effect on the overall trajectory. At present, the effect of higher shearing rates on grain saltation is being investigated.

6. Conclusion

High-speed motion-picture films of saltating flows were analysed using a Vanguard Motion Analyzer. A number of trajectories were obtained and compared with theoretical trajectories generated by integration of the equations of motion including only a drag-force term. It was found that the filmed particles consistently reached greater heights than those predicted by the theory. It was suggested that the most reasonable source for this apparent additional lift force is the Magnus effect associated with particle rotation. When terms accounting for the Magnus effect were included in the equations of motion, theoretical trajectories in much better agreement with the filmed ones were obtained. High particle spinning rates were required to produce these new trajectories.

An approximate technique for obtaining average lift-off and impact angles and velocities from the films was described. This technique involves the collection of a number of short random trajectory segments of particles leaving or returning to the surface. These segments are extrapolated back to the surface to obtain either lift-off or impact angles and velocities.

An analytical procedure for finding average trajectories for particles in saltating flows was described. This procedure requires a knowledge of the relationships between the impact and lift-off angles, velocities and rotational speeds of a particle. There appears to be little experimental data available from which to establish these relationships. To demonstrate the procedure simple expressions for these relationships were assumed.

This work was supported by the Planetary Geology Program Office, National Aeronautics and Space Administration. We also acknowledge the services performed by the Film Production departments of NASA Ames Research Center, and Iowa State University.

REFERENCES

ALLEN, J. R. L. 1970 *Physical Process of Sedimentation: an Introduction.* George Allen & Unwin.

ANDRES, R. M. 1970 The mechanics of dust lifting with particular emphasis on the planet Mars. Ph.D. dissertation, Library, St Louis University, St Louis, Missouri.

BAGNOLD, R. A. 1941 *The Physics of Blown Sand and Desert Dunes.* Methuen.

BAGNOLD, R. A. 1973 The nature of saltation and of 'bedload' transport in water. *Proc. Roy. Soc.* A **332**, 473–504.

CHEPIL, W. S. 1945 Dynamics of wind erosion. I. Nature of movement of soil by wind. *Soil Sci.* **60**, 305–320.

CHEPIL, W. S. 1958 The use of evenly spaced hemispheres to evaluate aerodynamic forces on a soil surface. *Trans. Am. Geophys. Un.* **39**, 397–403.

EINSTEIN, H. A. & EL-SAMNI, E. 1949 Hydrodynamic forces on a rough wall. *Rev. Mod. Phys.* **21**, 520–524.

ELLWOOD, J. M., EVANS, P. D. & WILSON, I. G. 1975 Small scale Aeolian bedforms. *J. Sediment. Petrol.* **45**, 554–561.

FRANCIS, J. R. D. 1973 Experiments on the motion of solitary grains along the bed of a water-stream. *Proc. Roy. Soc.* A **332**, 443–471.

GILBERT, G. K. 1914 Transportation of débris by running water. Department of the Interior, United States Geological Survey, Professional Paper no. 86, Washington, D.C. Government Printing Office.

IVERSEN, J. D., POLLACK, J. B., GREELEY, R. & WHITE, B. R. 1976 Saltation threshold on Mars; the effect of interparticle force, surface roughness, and low atmospheric density. *Icarus* **29**, 381–393.

MONIN, A. S. & YAGLOM, A. M. 1965 *Statistical Fluid Mechanics: Mechanics of Turbulence*, vol. 1, pp. 272–289. M.I.T. Press.

MORSI, S. A. & ALEXANDER, A. J. 1972 An investigation of particle trajectories in two-phase flow systems. *J. Fluid Mech.* **55**, 193–208.

RUBINOW, S. & KELLER, J. 1961 The transverse force on a spinning sphere moving in a viscous fluid. *J. Fluid Mech.* **11**, 447–459.

TOROBIN, L. B. & GAUVIN, W. H. 1959 Fundamental aspects of solid–gas flow. *Can. J. Chem. Engng* **37**, 129–141, 167–176, 224–276.

TOROBIN, L. B. & GAUVIN, W. H. 1960 Fundamental aspects of solid–gas flow. *Can. J. Chem. Engng* **38**, 142–153, 189–200.

TSUCHIYA, Y. 1970 On the mechanics of saltation of a spherical sand particle in a turbulent stream. *Kyoto Univ., Disaster Prev. Res. Inst., Bull.* **19**, (5), 52–57.

WHITE, B. R. 1975 Particle trajectories of saltating grains in terrestrial and Martian atmospheres. Ph.D. dissertation, Iowa State University, Ames.

WHITE, B. R., GREELEY, R., IVERSEN, J. D. & POLLACK, J. B. 1976 Estimated grain saltation in a Martian atmosphere. *J. Geophys. Res.* **81**, 5643–5650.

ZINGG, A. W. 1953 Wind tunnel studies of the movement of sedimentary material. *Proc. 5th Hydraul. Conf., Bull.* 24, *Univ. Iowa Studies in Engng*, pp. 111–135.